

U.S. DEPARTMENT OF COMMERCE
National Technical Information Service

AD-A025 387

A SOLID STATE DRAG ANEMOMETER USED TO
MEASURE VERTICAL WIND SHEAR

AIR FORCE INSTITUTE OF TECHNOLOGY

MAY 1975

167053

AD A 025387

The Pennsylvania State University
The Graduate School
Department of Meteorology

A Solid State Drag Anemometer Used to
Measure Vertical Wind Shear

A Paper in
Meteorology

by

George F. Duffield

Submitted in Partial Fulfillment
of the Requirements
for the Degree of
Master of Science

May 1975

DISSEMINATION STATEMENT A
Approved for public release
Distribution unlimited

Date of Approval:

May 29, 1975

John M. Norman
John M. Norman
Assistant Professor of Meteorology
Thesis Advisor

May 29, 1975

Alfred K. Blackadar
Alfred K. Blackadar
Head of the Department of Meteorology

REPRODUCED BY
NATIONAL TECHNICAL
INFORMATION SERVICE
U. S. DEPARTMENT OF COMMERCE
SPRINGFIELD, VA. 22161

ACKNOWLEDGEMENTS

The author wishes to express his sincere appreciation to Dr. John M. Norman for his assistance throughout this experiment and for the use of his equipment. In addition the author wishes to thank Dr. Niels Busch of the Danish AEC Risø for the materials and wind vane design; and Dr. David Martsolf for the use of his site and facilities.

NO.	DATE	TIME	TYPE	STATUS
			Wind Station <input checked="" type="checkbox"/>	
			Dist. Station <input type="checkbox"/>	
			Per <input type="checkbox"/>	
70m 1473				
REGISTRATION AVAILABILITY CODES				
NO.	DATE	TIME	TYPE	STATUS
A				

TABLE OF SYMBOLS

A	area (m^2)
b	width of steel strip supporting drag element (mm)
c	proportionality constant (dimensionless)
C_D	drag coefficient (dimensionless)
C_1	linear strain coefficient
C_2	non-linear strain coefficient
d	characteristic body dimension (m)
Δ	finite difference
E	voltage (volts)
e	modulus of elasticity
ϵ	strain = $\frac{\Delta l}{l}$ (dimensionless)
F	drag force (Newtons/ m^2)
g	gravitational acceleration (m/sec^2)
Γ	dry adiabatic lapse rate ($^{\circ}C/km$)
γ	environmental lapse rate ($^{\circ}C/km$)
h	height (m)
I	current (amps)
I_m	moment of inertia ($Kg-m^2$)
k	Von Karman constant (0.41)
l	length (m)
$\frac{\Delta l}{l}$	strain in steel strip (micrometers/meter)
v	kinematic viscosity ($0.15 \times 10^{-4} m^2/sec$ for air)
θ	potential temperature ($^{\circ}C$)
ρ	density (kg/m^3)
R	resistance (ohms)

TABLE OF SYMBOLS (continued)

r	radius (m)
R_o	reference level resistance (ohms)
R_f	Richardson Index (flux form) (dimensionless)
R_i	Richardson Index (gradient form) (dimensionless)
ΔR	change of resistance (ohms)
T_o	reference temperature ($^{\circ}\text{C}$)
T	temperature ($^{\circ}\text{C}$)
u	horizontal wind velocity component along x-axis (m/sec)
u_*	friction velocity (m/sec)
v	horizontal wind velocity component along y-axis (m/sec)
\vec{v}	wind vector (m/sec)
V	voltage (volts)
V_E	output signal for constant voltage circuit (volts)
V_I	output signal for constant current circuit (volts)
w	thickness of metal strip (mm)
z	height above ground (m)
z_o	roughness length (m)

A SOLID STATE DRAG ANEMOMETER USED TO MEASURE VERTICAL WIND SHEAR

1.0 INTRODUCTION

1.1 General Statement of the Problem

Micrometeorologists and air pollution meteorologists often require reliable indications of the vertical shear in the horizontal wind field in the planetary boundary layer. The vertical wind shear is an essential parameter of atmospheric stability and turbulent mixing. Accurate measurements of this quantity and vertical temperature gradients are combined to indicate atmospheric stability in terms of the gradient Richardson number. The gradient Richardson number is defined as the ratio of the rate of turbulent energy destruction by buoyancy forces to the rate of production of mechanical energy by wind shear. The most frequently used forms are:

$$(1) \quad Ri = \frac{\frac{g}{\theta} \frac{\partial \theta}{\partial z}}{\left(\frac{\partial u}{\partial z}\right)^2} = \frac{g}{\theta} \frac{(\Gamma - \gamma)}{\left(\frac{\partial u}{\partial z}\right)^2}$$

According to Slade (1968), "the Richardson number has come to be used as a characteristic turbulent parameter". Because accurate measurements of wind shear have been difficult to make, it has been necessary to obtain the Richardson number from approximations to vertical wind shear.

Budyko (1974) states that the Richardson number can be satisfactorily approximated in the surface layer by $\Delta T/u^2$. Fuchs and Tanner (1967) use the following form of the Richardson number to obtain the diabatic influence function in the planetary boundary layer:

$$(2) \quad Ri = \frac{\beta}{T} \left[\ln\left(\frac{z + z_0}{z_0}\right) \right] \left(\frac{T_z - T_0}{v_z^2} \right) z \quad ,$$

where the variables subscripted with z are measured at a selected height above the surface and T_0 is the soil surface temperature. Deacon uses the approximation

$$(3) \quad Ri = \frac{\theta_{5.0} - \theta_{0.2}}{\bar{u}_1^2} \quad ,$$

where the numerator gives the mean lapse rate of potential temperature in the layer 5.0 meters to 0.2 meter and \bar{u}_1 is the mean wind speed at 1 meter.

Measurements of the velocity gradient are more desirable than estimates especially if the instrumental technique is not overly involved. A satisfactory technique of applying the drag anemometer principle to sensors using high quality solid state strain gages results in an instrument which will accurately measure the velocity gradient. It is intended that this instrument be used operationally to measure Richardson number for air pollution and micrometeorological applications. When combined with existing

techniques for measuring vertical temperature gradients, it could be used to continuously monitor the Richardson number so that diffusion rates could be estimated in areas where toxic substances and hazardous materials are maintained. Measurements of the Richardson number obtained by this technique can be applied directly to Pasquill's recently revised method for calculating dispersion since his curves were developed in terms of Richardson number. The direct measurement of Richardson number, which is possible with this instrument, can thus provide a more precise and convenient method for determining stability and estimating dispersion than current methods estimating or measuring various fluxes.

1.2 Previous Studies in this Area

The drag anemometer is a simple device that is well suited for wind velocity measurements. The drag force resulting from wind flowing over a body causes deformation of a cantilever; the strain in this strip can be sensed by strain gages. Chepil and Siddoway (1959) were among the first to use strain gages with a drag anemometer. They fitted strain gages to pressure plate assemblies and used them to determine characteristics of the mean wind and turbulence. Since suitable commercial gages were not available at that time, wire filament strain gages were constructed by cementing constantan filament wire to a thin paper backing. Two pairs of these strain gages in a wheatstone bridge circuit were used to sense the force of the air against an aluminum pressure plate. Stress on these strain gages was directly proportional to the pressure of turbulent air

currents. Measurements were made at different heights over various surfaces in a wind tunnel and in the planetary boundary layer. Chepil and Siddoway give no threshold velocity for their instrument, but they do state that the highest frequency oscillation they were able to measure was 120 HZ.

Reed and Lynch (1963) used a series of drag sphere anemometers mounted on space vehicle launchers to measure instantaneous wind profiles and wind loading on space vehicles. Their drag sphere anemometers were designed to use two sets of strain gages to measure drag on a spherical body. They experimented with a "hole ball" (Wiffle ball) and a ping-pong ball for drag bodies. The "hole ball" had more desirable response characteristics than the smooth sphere. The smooth sphere exhibited what these researchers termed a "knuckle ball" effect due to vortex shedding and possible irregularities in its sphere. Reed and Lynch give no threshold velocities for their instruments, but it appears that most of their measurements were taken at high wind velocities.

Norwood, Cariffée, and Olszewski (1966) further refined the solid state, drag anemometer and used it to measure wind direction and velocity. They proposed an operational digital readout of averaged velocity and bearing. These researchers found that perforated spheres and lightweight plastic cylinders give best results for wind velocity measurements.

Pond, Smith, Hamblin and Burling (1966) used a "thrust anemometer", developed by L. A. E. Doe of the Bedford Institute of Oceanography, to measure the three dimensional wind vector in studies of velocity spectra

over a sea surface. A perforated spherical shell 9.6 cm in diameter was used as a drag body. Displacements of this body were transmitted mechanically to three sets of springs whose small displacements were sensed by differential transformers. This anemometer was designed for wind speeds in the range of 4 to 20 m/sec. Difficulties were encountered due to the extreme sensitivity of this instrument to oscillations of the mast it was mounted on. This anemometer did measure the $-5/3$ slope at higher wave numbers in the spectrum, but could not match the high response of a hot wire and was not quite as accurate as a sensitive cup anemometer.

More recent investigations have been made at The Pennsylvania State University by Norman. Solid state drag anemometers developed by Norman were used to construct the velocity gradient instrument used for this study. These devices are small, sturdy and relatively inexpensive. Styrofoam cylinders function as drag bodies and Wheatstone bridge circuitry is employed with solid state strain gages forming the active resistance elements of the bridge. At high Reynolds numbers, when air flowing over the cylinder is turbulent, drag forces exerted on the cylinder are proportional to the square of wind speed.

1.3 Specific Statement of the Problem

The goal of this research was to determine whether or not it is possible to accurately measure vertical gradients of horizontal velocity over short distances using the drag anemometer. When it was determined

to be feasible the objective was expanded to include construction and testing of an instrument which is suited for operational work in diffusion, turbulence and micrometeorology where measurements of the vertical wind shear are required. The gradient Richardson number, a very important operational stability parameter, can be obtained directly from this parameter and the vertical temperature gradient. Therefore, the instrument is designed to be easily modified to measure the Richardson number directly.

2.0 THEORETICAL DEVELOPMENT

2.1 Basic Theory of the Drag Anemometer

The basic principle of using the drag force of wind on an object to measure wind velocity dates back to Hooke's first anemometer of 1667. The equation describing kinematic drag force (F) on an object is

$$(4) \quad F = C_D A \rho V^2 / 2 \quad ,$$

where C_D is a coefficient depending on the shape and size of the drag body as well as the Reynolds number

$$(5) \quad Re = \frac{ud}{\nu} \quad .$$

The object used for a drag body is a right circular cylinder with a projected area

$$(6) \quad A = 2rh \quad .$$

The drag coefficient for this cylinder is given in Figure 2.1.1 as a function of Reynolds number and velocity. For the wind velocities we are considering the value of C_D will be about 1.0

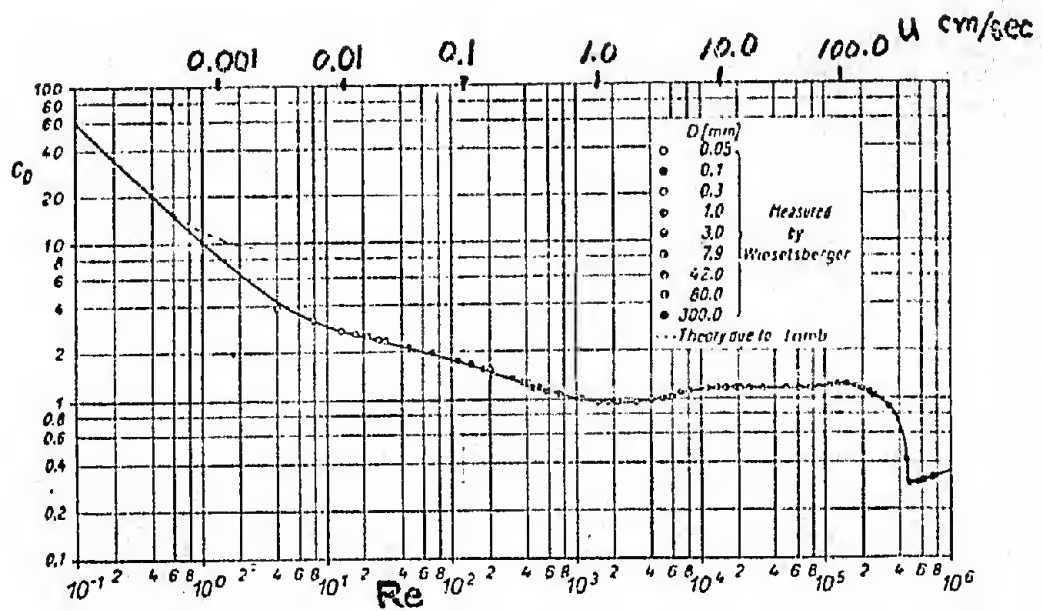


Figure 2.1.1. Drag coefficient given as a function of Richardson number and velocity.

Substituting equation (6) into equation (4) the drag force becomes

$$(7) \quad F = C_D r \rho V^2 .$$

The drag force acts along a cantilever fixed opposite the drag body as shown in Figure 2.1.2. A ceramic rod transmits drag forces to a metal strip, which serves as the primary cantilever. When the drag body experiences dynamic forces, the metal strip bends, resulting in strains that are sensed by strain gages mounted on this strip. By placing a strain gage on each side of the cantilever, sensitivity is increased and temperature effects are minimized. The strain of the cantilever shown in Figure 2.1.2 is

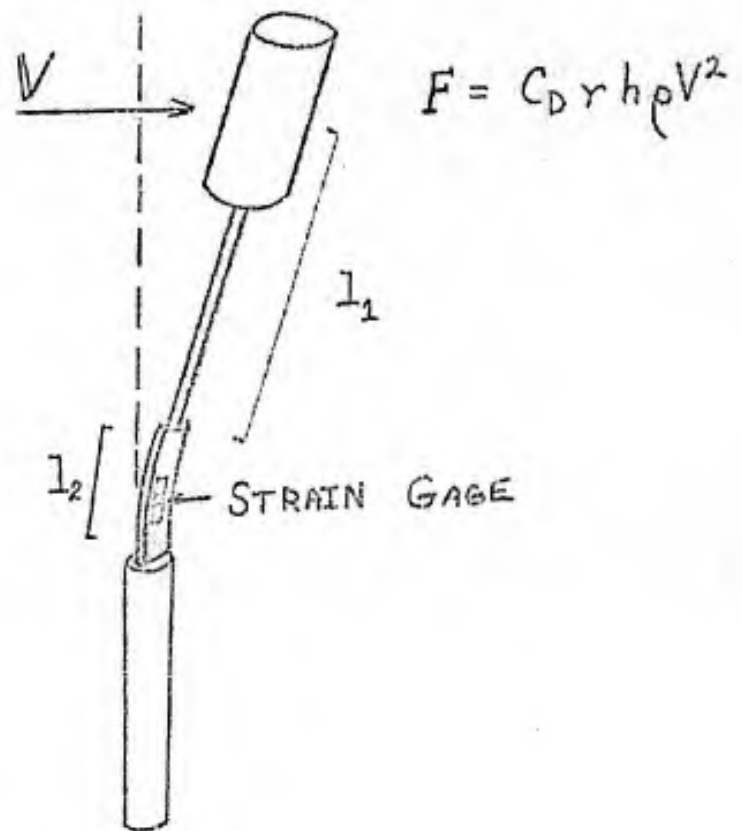


Figure 2.1.2. Deflection of the cantilever by the drag force, F , acting on the styrofoam cylinder. The resulting deformation of the metal strip is shown here with tension on the left of the strip and compression on the right.

$$(8) \quad \frac{\Delta l}{l} = \frac{Fb(l_1 + l_2/2)}{2eI_m}$$

where $I_m = wb^3/12$, l_1 is the length of the ceramic rod, and l_2 is the length of the metal strip. The strain gage pair will sense equal but opposite strains since one will be elongated when the other is compressed. The effect of the velocity in equation (8) is shown directly by substituting equation (7) to get

$$(9) \quad \frac{\Delta l}{l} = \frac{6[l_1 + l_2/2]}{ewb^2} C_D \rho V^2$$

The fact that strain is proportional to velocity squared leads to some complications in utilizing the strain gage anemometer as a sensor for measuring velocity gradients because of the nonlinear relation between velocity and output.

2.2 Theory of Velocity Gradient Measurements

The most convenient method for obtaining a finite difference form of the vertical gradient of horizontal velocity is to use drag anemometer outputs to sense velocity differences directly. Since the drag anemometer output is proportional to the square of horizontal wind speed, smaller differences in wind speed theoretically can be detected with greater precision than with instruments having a linear calibration curve. Some manipulation of signals is necessary before the velocity

gradient can be obtained from drag anemometer signals because the output is proportional to velocity squared. If the strains sensed by two drag anemometers mounted at different heights are differenced directly, the output is proportional to

$$(10) \quad u_2^2 - u_1^2 = (u_2 - u_1) (u_2 + u_1) \quad .$$

To obtain $\Delta u = u_2 - u_1$, equation (10) can be written as

$$(11) \quad u_2 - u_1 = \frac{u_2^2 - u_1^2}{u_2 + u_1} \quad ,$$

where $u_1 + u_2 = 2\bar{u}$, so that

$$(12) \quad u_2 - u_1 = \frac{u_2^2 - u_1^2}{2\bar{u}} \quad .$$

Equation (12) has the distinct advantage that differences in the numerator are directly proportional to drag anemometer output and this difference can be taken directly in a Wheatstone bridge circuit. Thus, it is possible to use three drag anemometers at different heights to measure differences in velocity by differencing directly two anemometers and dividing this quantity by the square root of a third unit mounted between the other two. Four strain gages, two on each of the differencing set of anemometers, form the four resistance elements of a fully active Wheatstone bridge.

The numerator is obtained when a strain gage in compression (tension) on the upper anemometer is paired directly opposite a strain gage in compression (tension) on the lower anemometer so that one bridge output registers differences in strain directly. This circumvents the nasty problem of differencing two large numbers that are nearly equal and results in improved precision in the velocity difference. The only constraint is that strain gage pairs for the two drag elements must be reasonably well matched for this to work. A typical half active bridge application is used to obtain the denominator and the output is processed to obtain the square root. Schematically the sensors are arranged as shown in Figure 2.2.1 below.

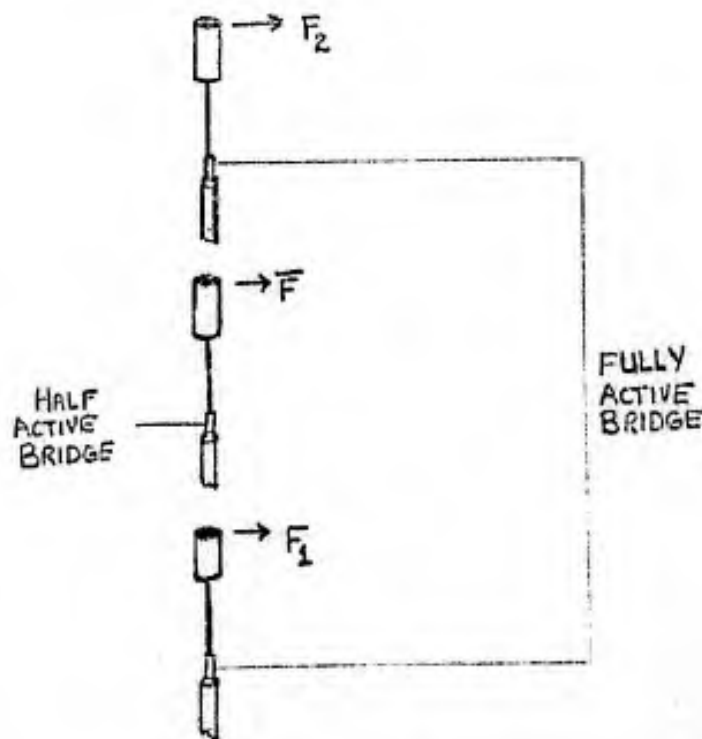


Figure 2.2.1. Arrangement and output of the three drag anemometers.

Thus, drag forces are sensed at three levels by three pairs of strain gages and their signals are transformed by two Wheatstone bridge circuits to directly produce velocity differences.

2.3 Basic Strain Gage Theory

Strain gages serve as transducers in the solid state drag anemometer. As stated previously, these are mounted in pairs on each anemometer so that one strain gage senses compression on the metal strip while the other senses tension. The strain gages' resistance changes proportionally to the tension or compression, which is in turn proportional to the drag force of wind acting on the drag body. The resistance changes are proportional to the stress such that

$$(13) \quad \frac{\Delta R}{R} = c \frac{\Delta l}{l} ,$$

where the proportionality constant c is on the order of 2 to 3 for wire type strain gages and about 100 to 150 for solid state strain gages. Semiconductor strain gages thus require less amplification than wire or filament gages and because they are able to sense much smaller strains, a smaller percent error exists in signals due to electrical noise.

Semiconductor strain gages take advantage of piezoelectric properties of crystalline substances such as silicon. Resistance of piezoelectric substances changes as the material is subject to different amounts of compression or elongation. According to Dorsey (1964), silicon is the best piezoelectric material for Wheatstone bridge applications. This semiconductor strain gage does have one distinct drawback; its resistance also depends on temperature. This deficiency can be overcome by modifying the bridge circuit for many applications.

Two types of semiconductor strain gages are available commercially - the N-type and P-type. The N-type has its measurement axis oriented one-dimensionally along the crystal axis. It is designed to compensate for temperature induced zero shifts when bonded to certain specimen materials. It is an ideal choice for applications requiring only one strain gage. The P-type strain gage is used in Norman's drag anemometer sensors because it is desirable to use strain gage pairs to increase sensitivity. In general, P-type strain gages are more linear, more sensitive, and have less absolute sensitivity change with temperature than the N-type gage. Bulk, P-type (silicon) semiconductor strain gages, mounted in opposing pairs, were considered best suited for this drag anemometer application.

The basic equation describing resistance change in semiconductor strain gages is:

$$(14) \quad \frac{\Delta R}{R} = \left(\frac{T_0}{T}\right) C_1 \epsilon + \left(\frac{T_0}{T}\right)^2 C_2 \epsilon^2 \quad ,$$

where T_0 is the reference temperature ($^{\circ}\text{K}$) and T is the actual temperature. When the ratio T_0/T is unity equation (14) reduces to

$$(15) \quad \frac{\Delta R}{R} = C_1 \epsilon + C_2 \epsilon^2 \quad .$$

According to Brackett (1968), if we substitute this form of the equation into a Wheatstone bridge circuit, which is fully active with two of four identical strain gages in compression and two in tension, we can determine circuit properties. Brackett (1968) goes on to state that a constant current circuit is generally superior because of its exactly linear output signal

$$(16) \quad V_I = IRC_1 E \quad ,$$

where I is the circuit excitation current. A constant voltage circuit has a signal output

$$(17) \quad V_E = \frac{E C_1 \epsilon}{1 + C_2 \epsilon^2} \quad ,$$

where E is the circuit excitation voltage. Thus, we are faced with a non-linear effect for a constant voltage Bridge circuit. Fortunately, this effect is negligible since

$$(18) \quad c_2^2 \ll 1$$

and the squared term in equation (17) may be neglected. Brackett (1968) states that this approximation results in less than a 0.25 percent error for strains less than 1000 microstrain (micrometers/meter). In drag anemometers the strain is much smaller and this approximation is even better. This is fortunate because a constant voltage source is considered to be more convenient than a constant current source for this application.

The greatest obstacle to this application arises from the temperature coefficient of P-type solid state strain gages. P-type semiconductor strain gages display sensitivity decreases while exhibiting resistance increases with increasing temperature. Temperature compensation for individual anemometers is accomplished by mounting a thermistor near the strain gages and using its output to modify the circuit. If the temperature coefficients of the differencing drag anemometers are constant, compensation can be done by using the temperature difference between the strain gages pairs. Alternatively, the temperature of each strain gage pair can be monitored and the velocity difference corrected during data processing. Temperature effects can be minimized by mounting the strain gages so that the thermal gradient is very small between each pair. This usually involves mounting the gages as closely as possible while maintaining symmetry in the pair. This requirement is especially important

for full bridge applications, where all resistors are strain gages. These principles were adhered to strictly when strain gage pairs were mounted on stainless steel strips. Some differences in drag element characteristics did arise due to different types of cements being used. Epoxy cement and contact cement were used to mount the various strain gage pairs onto the stainless steel strips. The contact cement was faster drying, but was not as permanent as epoxy. Although they were permanent and more weather resistant, the epoxy gages did exhibit some hysteresis effects.

2.4 Basic Theory of Bridge Circuits

The Wheatstone bridge is one of the most useful and frequently employed electronic circuits for instrumentation according to Norman and Thomson (1974). It can be used to compare unknown resistances or to convert resistance changes to signals of either current or voltage. The Wheatstone bridge circuit is shown schematically in Figure 2.4.1 below.

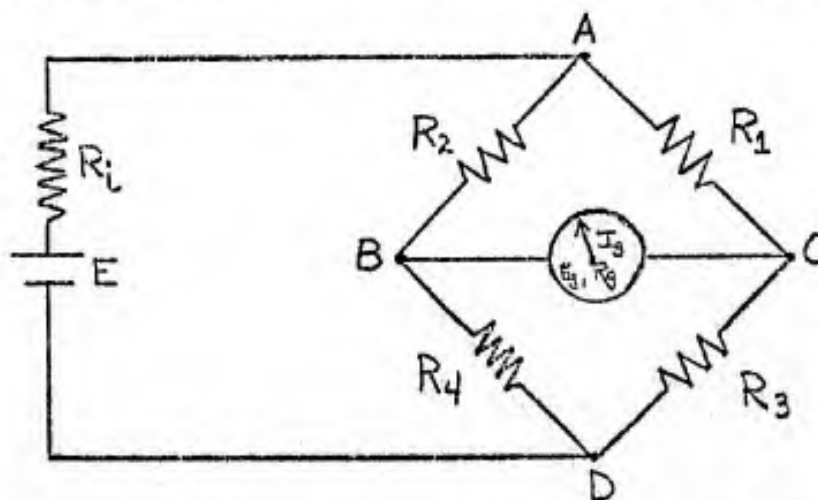


Figure 2.4.1. Wheatstone bridge circuit, where R_1 , R_2 , R_3 and R_4 are resistance arms of the bridge; E , R_i and I_g are voltage across the gage resistance and gage current; E is electromotive force of the battery, and R_i is the battery resistance.

The Wheatstone bridge circuit is said to be "balanced" when no current or voltage is sensed across the meter or equivalently there is no flow between points B and C so that $E_g = 0$ or $I_g = 0$. In a "balanced" state the circuit resistances are related by

$$(19) \quad \frac{R_1}{R_3} = \frac{R_2}{R_4} \quad .$$

Anytime a current or voltage is sensed across the bridge arms between points B and C, the bridge is said to be unbalanced. The equation for the voltage across an unbalanced bridge is given by Tanner (1956) as

$$(20) \quad E_g = \frac{E R_g (R_2 R_3 - R_1 R_4) / R_s}{(R_a) / (R_b) - R_c^2}$$

where

$$R_s = R_1 + R_2 + R_3 + R_4$$

$$R_a = \frac{(R_1 + R_2) (R_3 + R_4)}{R_s} + R_g$$

$$R_b = \frac{(R_2 + R_4) (R_1 + R_3)}{R_s} + R_1 \quad , \text{ and}$$

$$R_c = \frac{R_2 R_3 - R_1 R_4}{R_s} \quad .$$

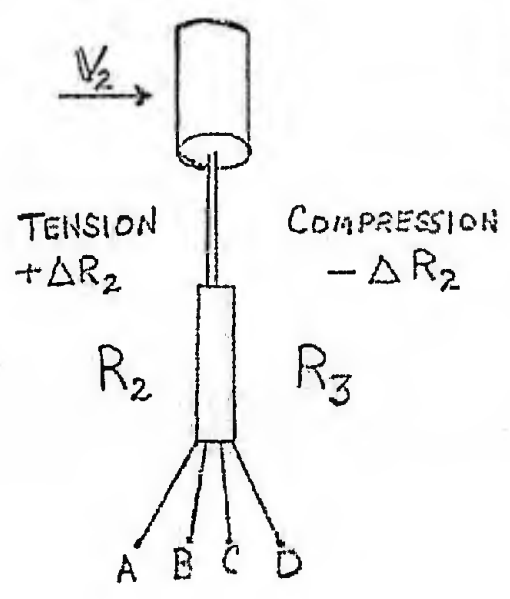
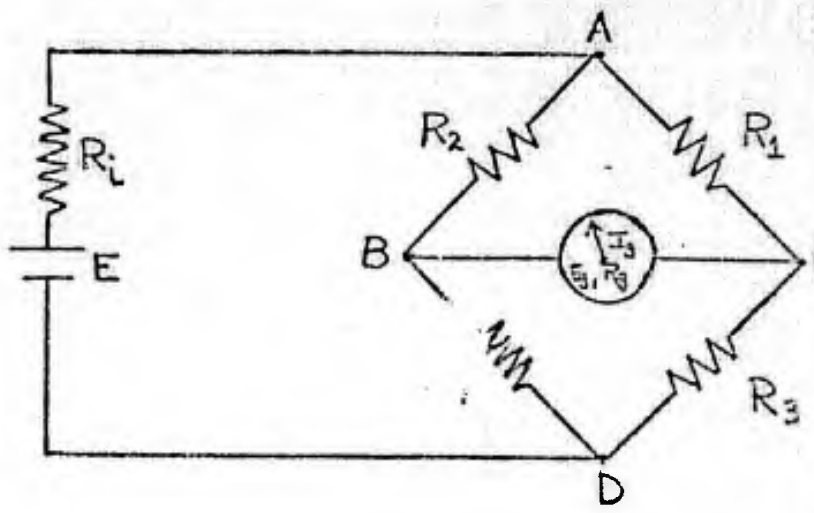
Maximum voltage sensitivity for an unbalanced bridge is achieved when the meter resistance is very large (compared to circuit resistances) and the voltage supply resistance R_1 is negligible. Under these conditions equation (2) becomes

$$(21) \quad E_g = \frac{E(R_2 R_3 - R_1 R_4)}{(R_2 + R_4)(R_1 + R_3)}$$

This is the working equation for the drag anemometer. The effects of the non-linearity arising from the square term in the semi-conductor strain gage equation were discussed earlier and found to be negligible.

In this application two pairs of strain gages from the differencing drag anemometers form a fully active bridge and the two strain gages of the averaging drag anemometer along with two precision resistors form a second bridge. Equation (21) is used to determine whether a "cross" bridge or "end" bridge application would be best suited for the full bridge. The "cross" bridge is when opposite diagonals are used for drag anemometer strain gage pairs as is illustrated in Figure 2.4.2. This is when R_1 and R_4 serve as a strain gage pair for one drag anemometer, while R_2 and R_3 serve as components of the other. This arrangement results in an output of

$$(22) \quad E_g = \frac{E(\Delta R_2^2 - \Delta R_1^2)}{4R_o^2 - \Delta R_1^2 - \Delta R_2^2 + 2\Delta R_1 \Delta R_2}$$



$$R_1 = R_0 + \Delta R_1$$

$$R_2 = R_0 + \Delta R_2$$

$$R_3 = R_0 - \Delta R_2$$

$$R_4 = R_0 - \Delta R_1$$

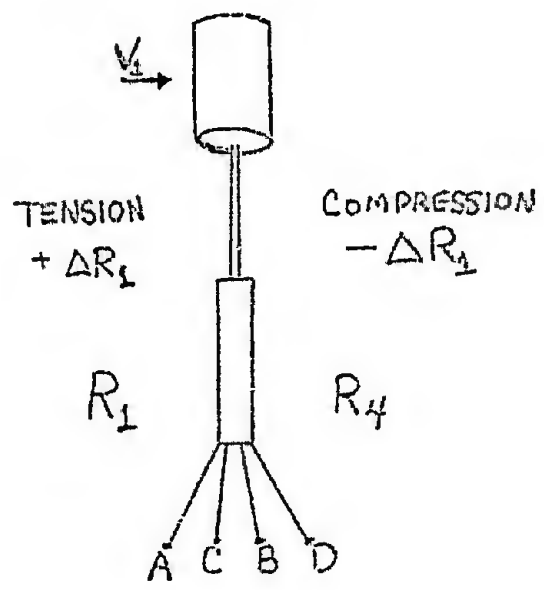


Figure 2.4.2. "Cross" Bridge.

where ΔR is the resistance change of a gage. This is undesirable since we have the difference of the squares of the two resistance changes.

The "end" bridge application is illustrated in Figure 2.4.3. It is when the top half of the Wheatstone bridge is composed of the strain gage pair on the upper anemometer and the bottom half bridge is composed of the strain gages on the lower anemometer. After substitution into equation (21) it is clear that the end bridge is best for this particular full bridge application since

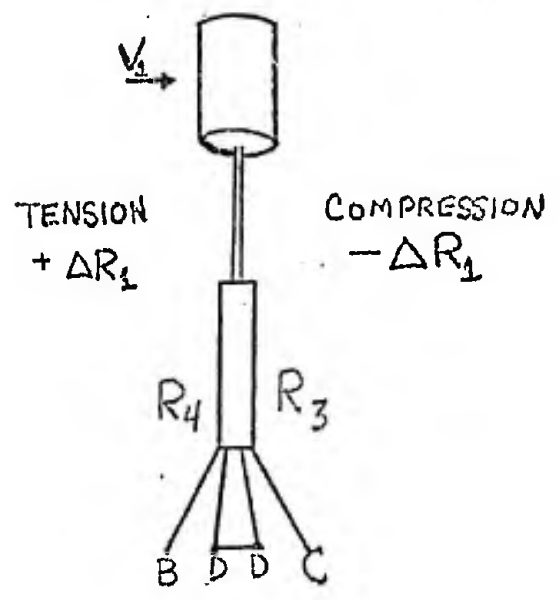
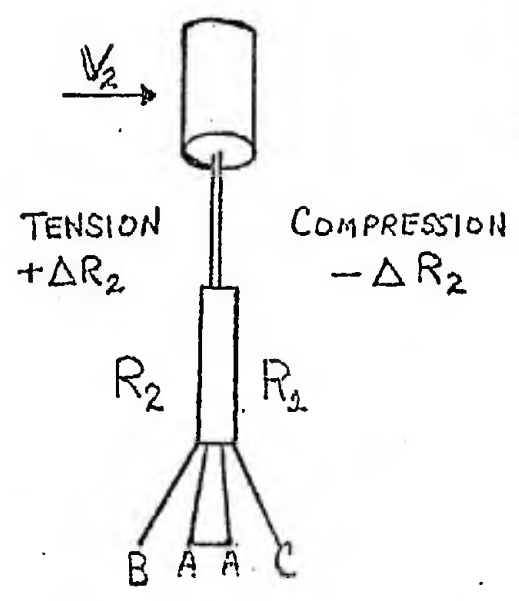
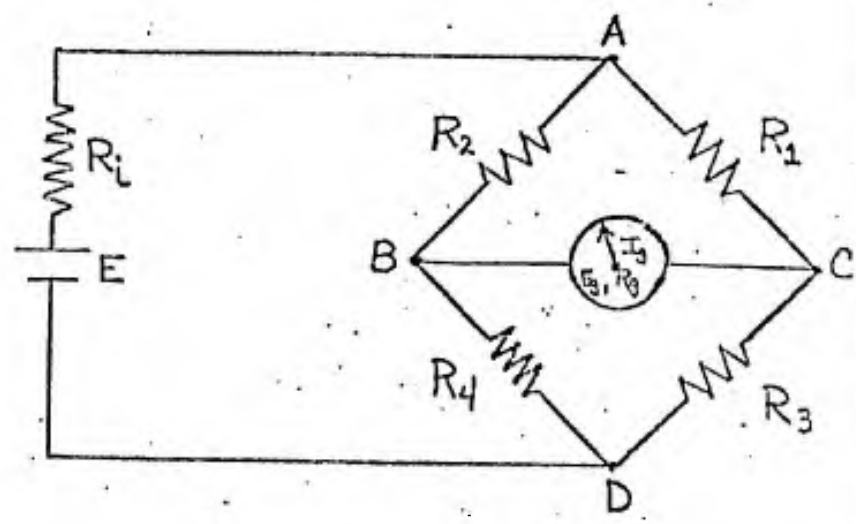
$$(23) \quad E_g = \frac{2R_o E [\Delta R_2 - \Delta R_1]}{4R_o - \Delta R_1^2 - \Delta R_2^2 - \Delta R_1 \Delta R_2}$$

This can be simplified, since the values of resistance change for each of the strain gages are nearly equal and much smaller than R_o , to yield

$$(24) \quad E_g = \frac{E[\Delta R_2 - \Delta R_1]}{2R_o}$$

The assumption that $(\Delta R)^2 \ll R_o^2$ results in less than 1 percent error in the difference of the upper and lower anemometers.

A side bridge application is used for the center drag anemometer where R_2 and R_4 are active bridge arms composed of the strain gages, while R_1 and R_3 are fixed precision resistors. The output of this circuit is



$$R_1 = R_0 - \Delta R_2$$

$$R_2 = R_0 + \Delta R_2$$

$$R_3 = R_0 - \Delta R_1$$

$$R_4 = R_0 + \Delta R_1$$

Figure 2.4.3. "End" Bridge.

$$(25) \quad E_g = \frac{E \Delta R}{2R_o} \quad .$$

2.5 How the Velocity Gradient Instrument may be Adapted to Measure the Richardson Number

The velocity gradient instrument may be adapted for direct measurements of gradient Richardson number by adding a capability to measure vertical temperature gradient. There are many available techniques and sensors for accomplishing this. Thermistors, diodes, thermocouples, or wire resistance thermometers could be used for these measurements. An excellent discussion on these sensors and their application is given by Tanner (1956). The particular sensors selected could be mounted on, or in the immediate proximity of, the three drag bodies so that the upper and lower sensors are used to measure temperature difference and the middle sensor used to measure average temperature. Thus, in finite difference form we would have all measurements necessary for the Richardson number

$$(26) \quad Ri = \frac{g}{\bar{\theta}} \frac{\Delta\theta/\Delta z}{[(\Delta u/\Delta z)]^2} \quad .$$

Combination of these electrical signals could provide a direct output of Richardson number.

3.0 DESCRIPTION OF THE INSTRUMENT

The velocity gradient instrument uses three drag anemometers mounted on sensitive wind vanes (Figure 3.1). These assemblies are constructed identically except for the use of unbacked strain gages in the center sensor and backed strain gages in the other two. All three drag anemometer assemblies are mounted on bases with leveling screws so that gravitational effects on the assembly are negligible. Thus, only drag forces acting on the styrofoam drag body are sensed. The drag body is a right cylinder 1.7 cm in diameter and 4.9 cm in height. A 0.18 cm diameter ceramic rod is used to transmit the drag force through a distance of 10.2 cm to the stainless steel strip (0.3 mm thick, 7.5 mm wide and 25 mm long) where the force is sensed by strain gages. Two Baldwin-Lima-Hamilton (BLH), 350 ohm, P-type silicon strain gages are mounted symmetrically opposed on the stainless steel strip. The gage factor, C' in equation (9), is 118 for both backed and unbacked strain gages. These specifications can be used to determine the theoretical output from a drag anemometer by a combination of equations (9), (13), and (25) to obtain

$$(27) \quad \frac{\Delta R}{R_o} = C' \frac{\Delta l}{l} \frac{6C'[1_1 + 1_2/2] C_D \rho u^2}{ewb^2} ,$$

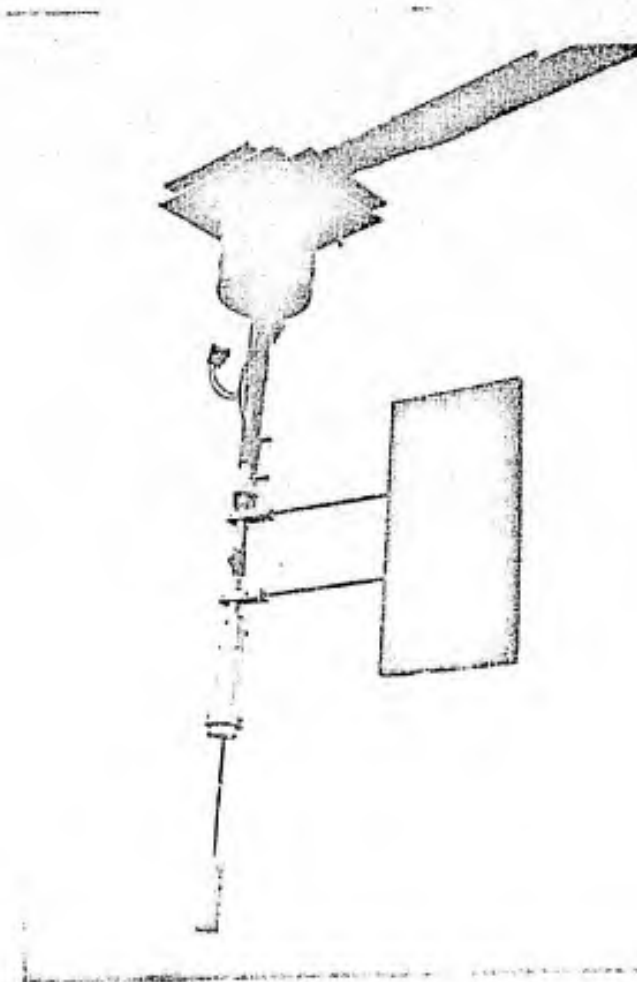


Figure 3.1. An individual sensor unit of the velocity gradient instrument consists of a drag anemometer mounted on a very sensitive wind vane. The assembly base is supported by a leveling system similar to that used in a transit.

where e is the bulk modulus of stainless steel ($2.067 \times 10^{11} \frac{\text{cm gm}}{\text{sec}}$). A typical half active, side bridge application with a constant excitation voltage has a signal

$$(28) \quad E_g = \frac{E}{2} \left\{ \frac{6C' [1_1 + 1_2/2] C_D rh \rho u^2}{ewb^2} \right\}$$

If we assume a density of $1.2 \times 10^{-3} \text{ gm/cm}^3$ and substitute appropriate values for the above constants equations (28) reduces to

$$(29) \quad E_g (\text{mv}) = \left\{ 2.90 \times 10^{-5} \frac{\text{mv}}{(\text{cm/sec})^2} \right\} u^2 C_D$$

A plot of the theoretical output is given for amplification with a gain of 140 in Figure 3.2.

Each sensor unit was calibrated against a hot wire anemometer at wind speeds ranging from 0 to 10 m/sec in a wind tunnel. These results yielded outputs which were a constant factor of 2 greater than those anticipated from theory (Figure 3.3). Sensors numbers 1 and 2 were chosen for the fully-active bridge application since their slopes and intercepts were closely matched. The inverse of the slopes as plotted in Figure 3.3 was used to obtain wind velocity from output.

The effects of temperature on the drag anemometer outputs was measured by copper-constantan thermocouples bonded to the stainless steel strips. This is necessary for measurements made over extended

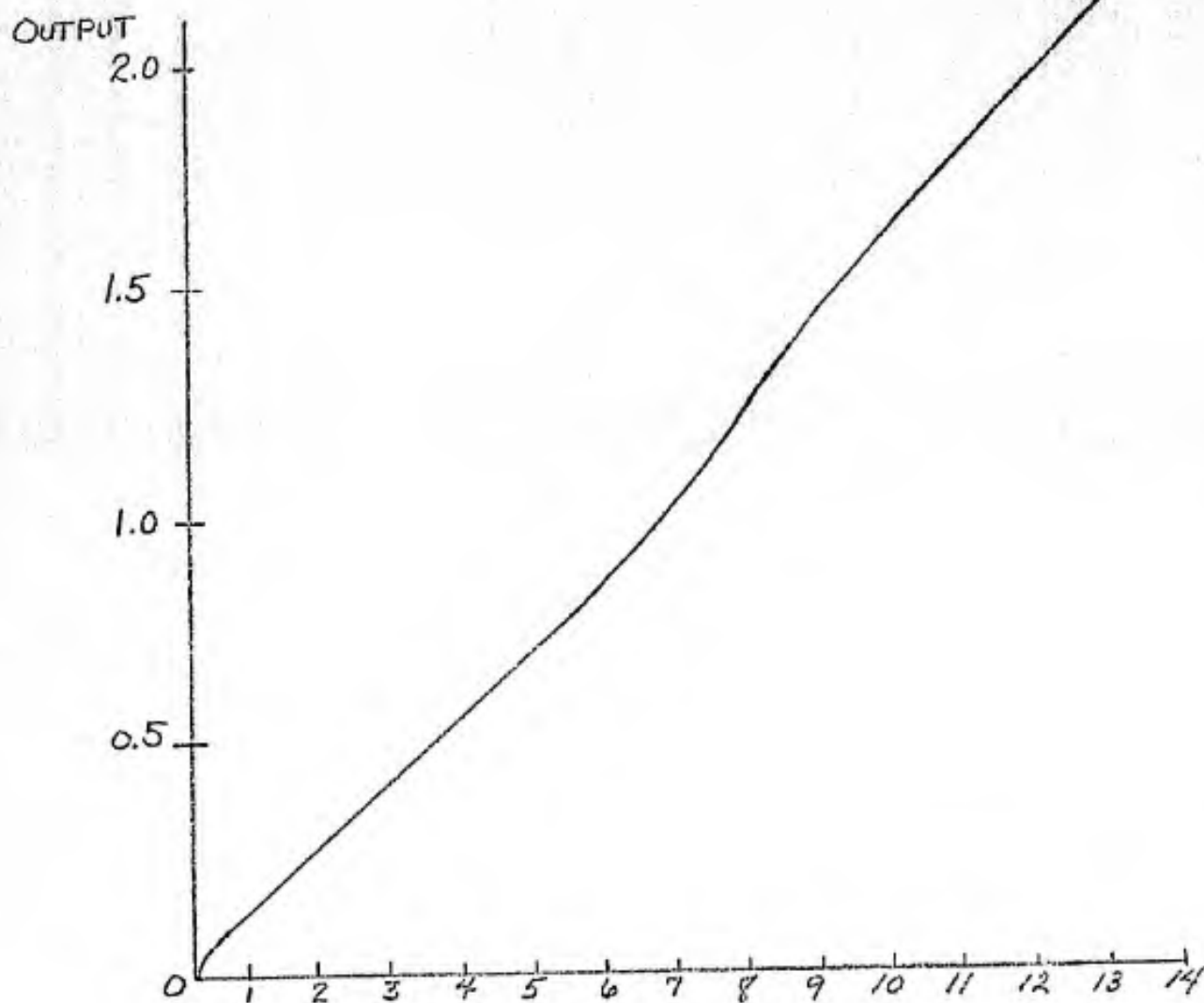


Figure 3.2. Plot of theoretical output for a half-active Wheatstone bridge formed using a single drag anemometer. Deviations from a fully linear system in this representation are due to variation of the drag coefficients with velocity.

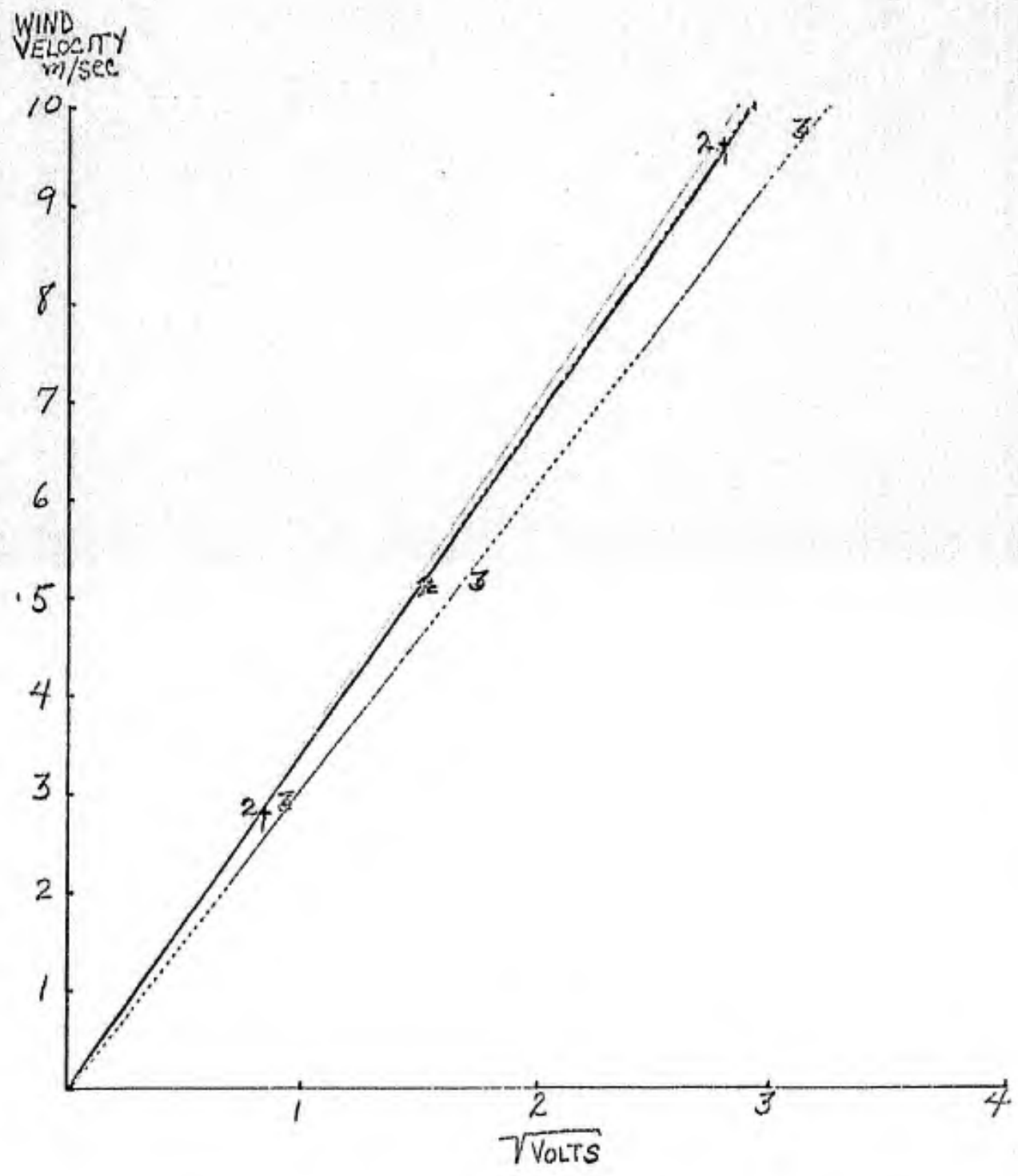


Figure 3.3. Calibration curves for the three sensors used in the velocity gradient instrument. A hot wire anemometer was used to calibrate the three sensors during runs in a wind tunnel.

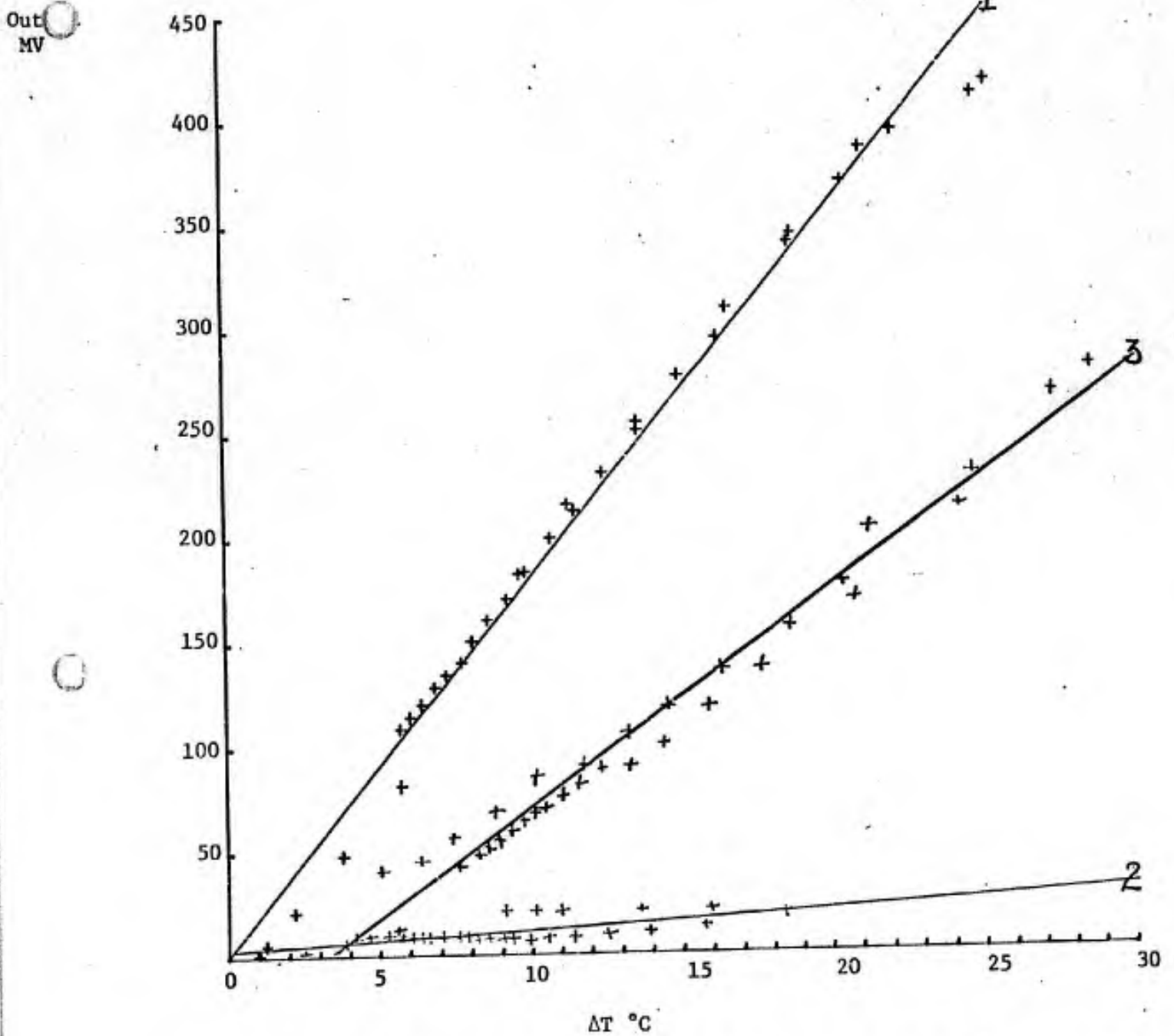
STRAIN GAGE
OUTPUT *mv*

Figure 3.4. Temperature coefficients were obtained using a least squares linear-regression technique. The temperature coefficients were:

$$C_1 = 17.85 \frac{\text{mv}}{^{\circ}\text{C}}, C_2 = 1.36 \frac{\text{mv}}{^{\circ}\text{C}}, \text{ and } C_3 = 7.92 \frac{\text{mv}}{^{\circ}\text{C}}.$$

time periods even though the effects of wind and radiation have been minimized with shielding. Temperature coefficients were determined for the three sensor pairs over a range of between 20°C and 40°C (Figure 3.4). Since all drag anemometers were within 0.6°C of each other during field tests, these temperature corrections were negligible. In an operational instrument automatic temperature compensation can be achieved by using thermistors in appropriate compensation circuits.

Each drag anemometer is mounted on a sensitive wind vane so that total drag force on the cylinder is always sensed by the strain gages. Weather Measure Corporation W103 cup anemometer bases were chosen for the vane supports, bearings, and shafts because of their low friction. The wind vane was designed by Busch and Larsen (1974), of the Meteorology Section of the Danish AEC Research Establishment Risø. The vane, which is critically damped and designed to operate without vibration at speeds up to 20 m/sec, consists of a flat polystyrene sheet (dimensions 0.7 x 10 x 20 cm) for an airfoil and arms of small, lightweight monel rods (20 cm in length) that extends from the support through the polystyrene sheet. The difference in colors noted on the wind vanes pictured in this paper is due to a coat of protective paint on the top vane. This coating makes the polystyrene extremely weather resistance, but does not significantly affect its response characteristics. The problem of sensing rotationally induced wind velocities is eliminated by mounting the drag body directly over the axis of rotation. The completed velocity gradient

instrument spans a distance of 1.9 m as it was configured for these tests (Figure 3.5). The supports are parallel to and facing into the mean wind so that the drag bodies are 0.9 m upwind and slightly to the side of the supporting structure.

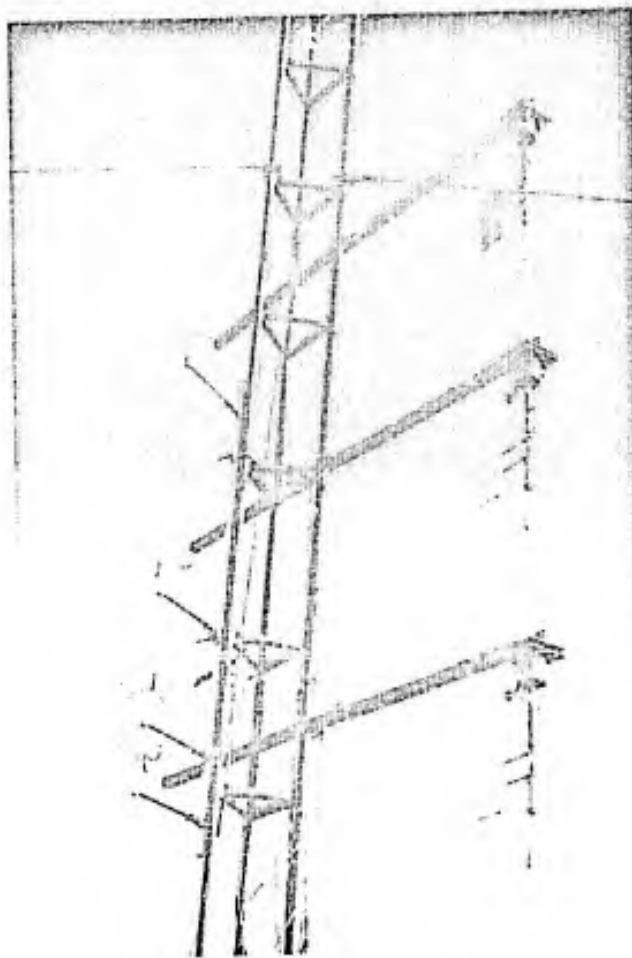


Figure 3.5. The velocity gradient instrument mounted for field testing. Note the Thornthwaite sensitive cup anemometer mounted to the left side of the tower.

4.0 TEST MEASUREMENTS, RESULTS AND CONCLUSIONS

The velocity gradient instrument was field tested against Thornthwaite sensitive cup anemometers (threshold speed = 9 cm/sec) to obtain an assessment of their comparability (Figure 4.1). One minute mean wind profiles were obtained over successive 10 minute periods using Thornthwaite anemometers, which are located 2.8 m, 3.0 m, 3.4 m and 4.2 m above the ground. Since the drag elements could not be located at precisely the same height as the cups, the mean profiles from the cup anemometers were plotted on semi log paper and extrapolated downward a distance of 9 cm to the height of the lower drag element and upward 33 cm to the height of the upper drag element. The two signal outputs from the three drag anemometers, located at 2.79 m, 3.69 m and 4.53 m above the ground, were recorded on a multichannel strip chart recorder with inputs filtered by an R-C low pass filter combination to provide a time constant of 0.3 seconds.

The oscillograph recordings were processed by averaging each signal over 3.75 seconds, applying corrections for the recorder calibrations, and calculating the velocity gradient from the following equation:

$$(30) \quad \frac{\frac{E_1}{a_1^2} - \frac{E_2}{a_2^2}}{\frac{\sqrt{E_3}}{a_3}} \cong \frac{\frac{\Delta E_{1,2}}{(\bar{a}_{1,2})^2}}{\frac{\sqrt{E_3}}{a_3}} - \frac{a(a_1 - a_2)}{\bar{a}_{1,2}} \frac{\sqrt{E_3}}{a_3}$$

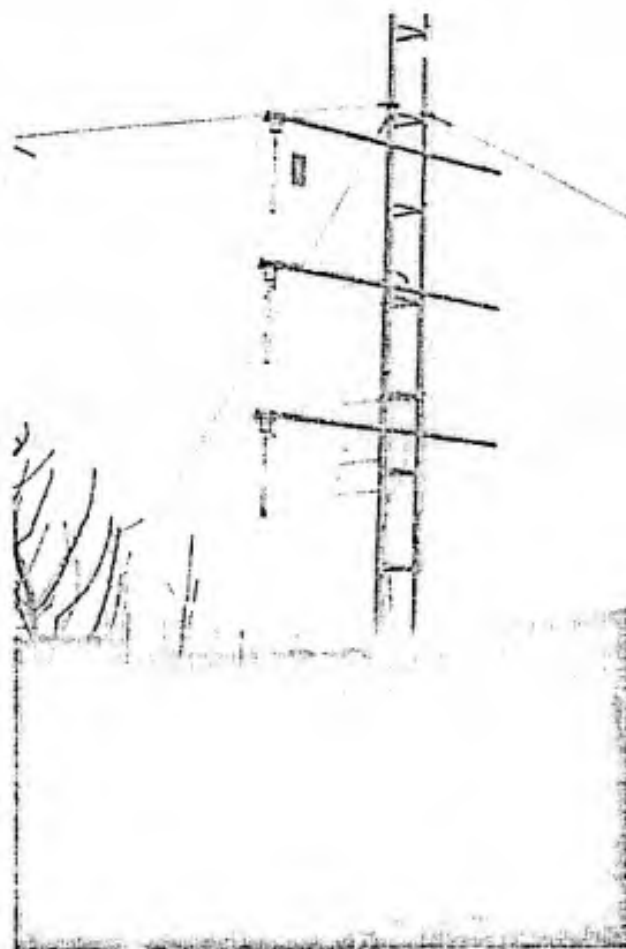


Figure 4.1. Horticulture Department site of measurements showing mast and instruments in relation to local terrain and obstructions. The drag elements are covered so that precise zero values can be obtained. The tallest trees surrounding the tower were about 1.2 m and were located not closer than 5.5 m to the tower or to other trees.

where $\Delta E_{1,2}$ is the signal from the velocity difference unit, E_3 is the center drag anemometer signal, $\bar{a}_{1,2}$ is the average slope of the calibration curve for sensor 1 and 2, and a_3 is the slope of the calibration curve for sensor 3. In the field tests the second term in equation (30) is small because $a_1 \approx a_2$ and $\Delta E_{1,2}$ are quite large.

The velocity gradient instrument was field tested during the afternoon of April 9, 1975, at The Pennsylvania State University, Horticulture Department orchard experimental site. A strong synoptic scale high pressure system centered over northern New York state dominated meteorologic conditions during the test period. A strong northwesterly flow of cool air from this high pressure region was passing over surfaces heated by strong solar insolation. A cirrostratus layer moved into the area throughout the afternoon increasing the cloud cover from 5/10 thin broken at 1400 EDT to 8/10 thin broken by 1530 EDT. Wind velocities averaged from 5 to 7 m/sec throughout this period. From these conditions one can easily surmise that stability was also increasing. Ambient air temperature hovered at about 12°C during the afternoon. From the conditions one expects the velocity gradient to increase with time.

Velocity differences over the interval 4.5 m to 2.7 m and velocity at 3.6 m, measured by the velocity gradient instrument, are given for 10 minute periods beginning at 1420 EDT in Figure 4.2a and at 1510 EDT in Figure 4.2b. The wind speed and velocity differences increased in the latter data set as was expected. The 10 minute average velocity was

4.83 m/sec during the first run and 6.44 m/sec during the latter. The range of 3.75 second average velocities was 2.91 m/sec to 8.39 m/sec during the first run and 3.66 m/sec to 10.4 m/sec during the second test. It is interesting to note the apparent phase relation between the velocity and velocity difference as plotted in Figures 4.2a and 4.2b. Generally the velocity difference is largest for lower wind speeds and least for greater wind speeds.

Readings of Thornthwaite cup anemometer counters were processed to obtain velocities and from this data wind profiles were plotted. Since the output of Thornthwaite anemometers was read from mechanical counters, while the runs progressed, considerable difficulties arose in obtaining accurate instantaneous readings for 1 minute mean profiles. When comparing data from the two instruments in Figures 4.3 and 4.4, limits of uncertainty due to extrapolation of Thornthwaite anemometer data to the drag heights are included. The 10 minute average velocity difference measured by the drag anemometers is 47.8 cm/sec compared to 44 cm/sec for the Thornthwaite anemometers during the 1420 EDT run. Results of the 10 minute velocity differences for the 1510 EDT run are 68.7 cm/sec from the drag anemometers versus 67.5 cm/sec measured by the Thornthwaite anemometers. These long term values are in excellent agreement.

A plot of scatter for the velocity differences measured by the two instruments is given in Figure 4.5. The problems with Thornthwaite data cause the large scatter for ΔV values, but the 10 minute mean ΔV values fall fairly close to the line of perfect correlation. Much of the

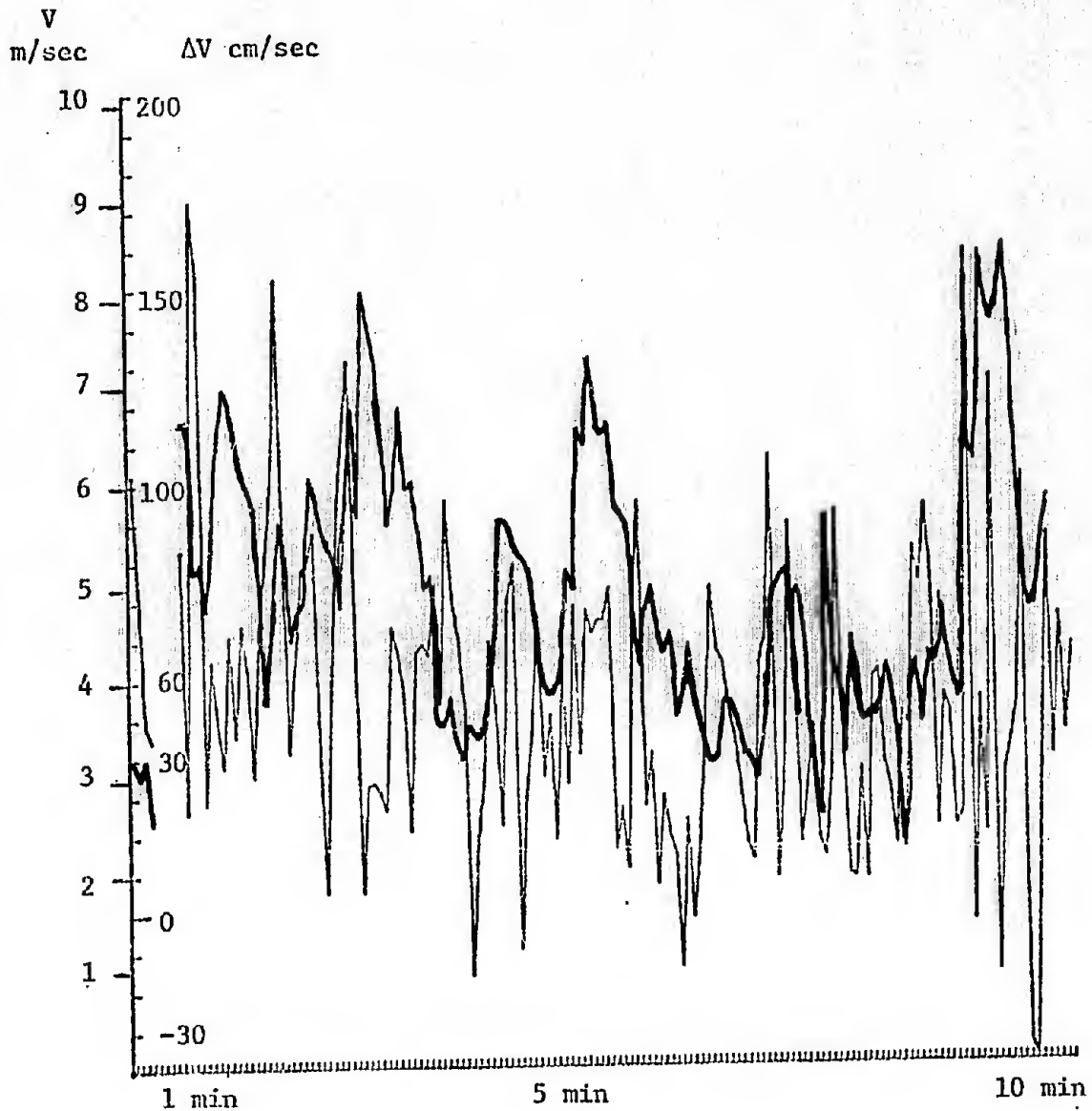


Figure 4.2a. Results of measurements taken during a 10 minute run beginning at 1420 EDT on April 9, 1975. Velocity gradient measured by the velocity gradient instrument is in black. Each value is averaged over a 3.75 second interval taken by hand from the oscillograph strip chart. Red profile is the 3.75 sec mean velocity taken at the center drag anemometer.

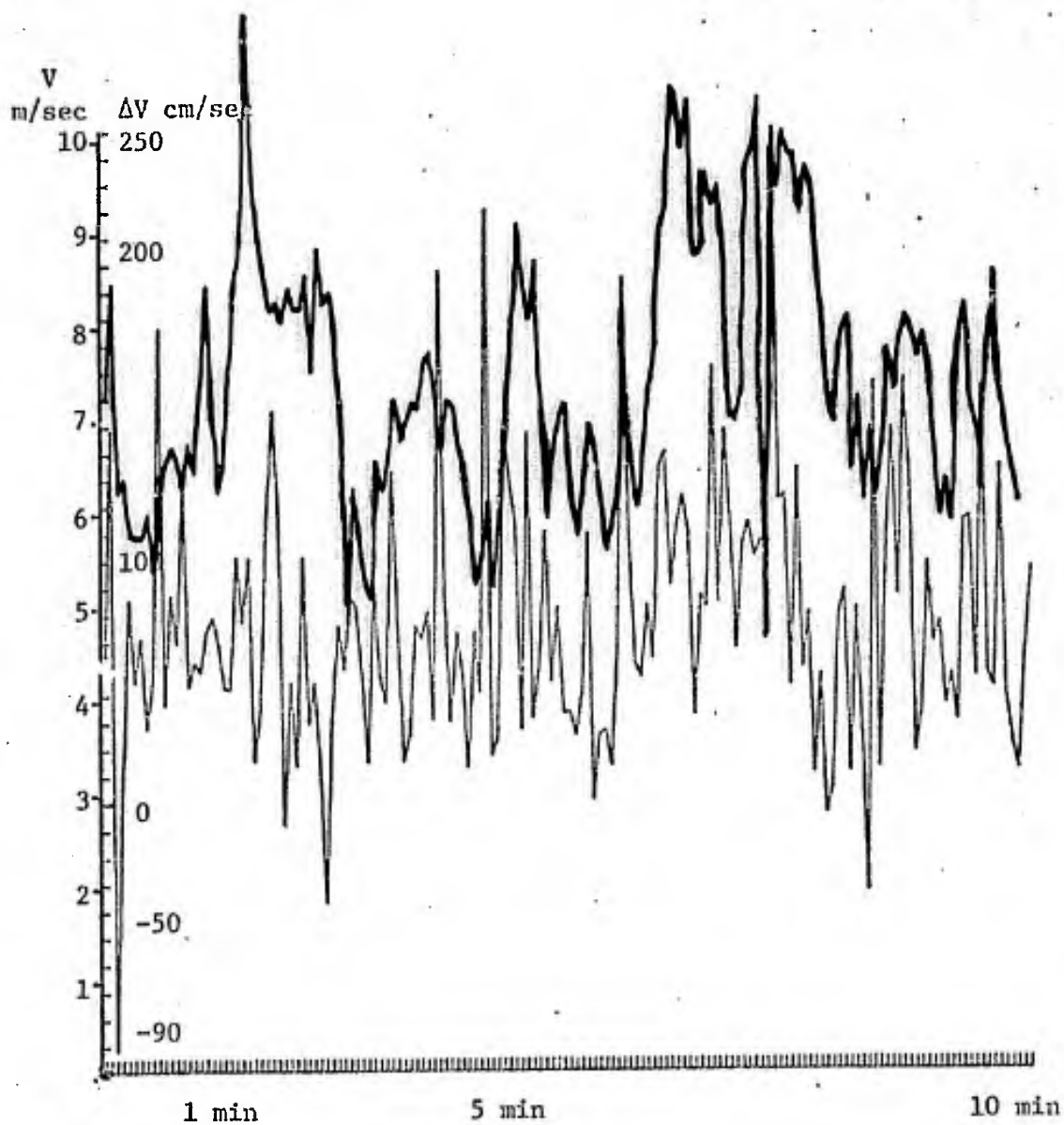


Figure 4.2b. Results of measurements taken during a 10 minute run beginning at 1510 EDT on April 9, 1975. Velocity gradient measured by the velocity gradient instrument is in black. Each value is averaged over a 3.75 second interval. The mean velocity measured at the center drag anemometer is plotted in red.

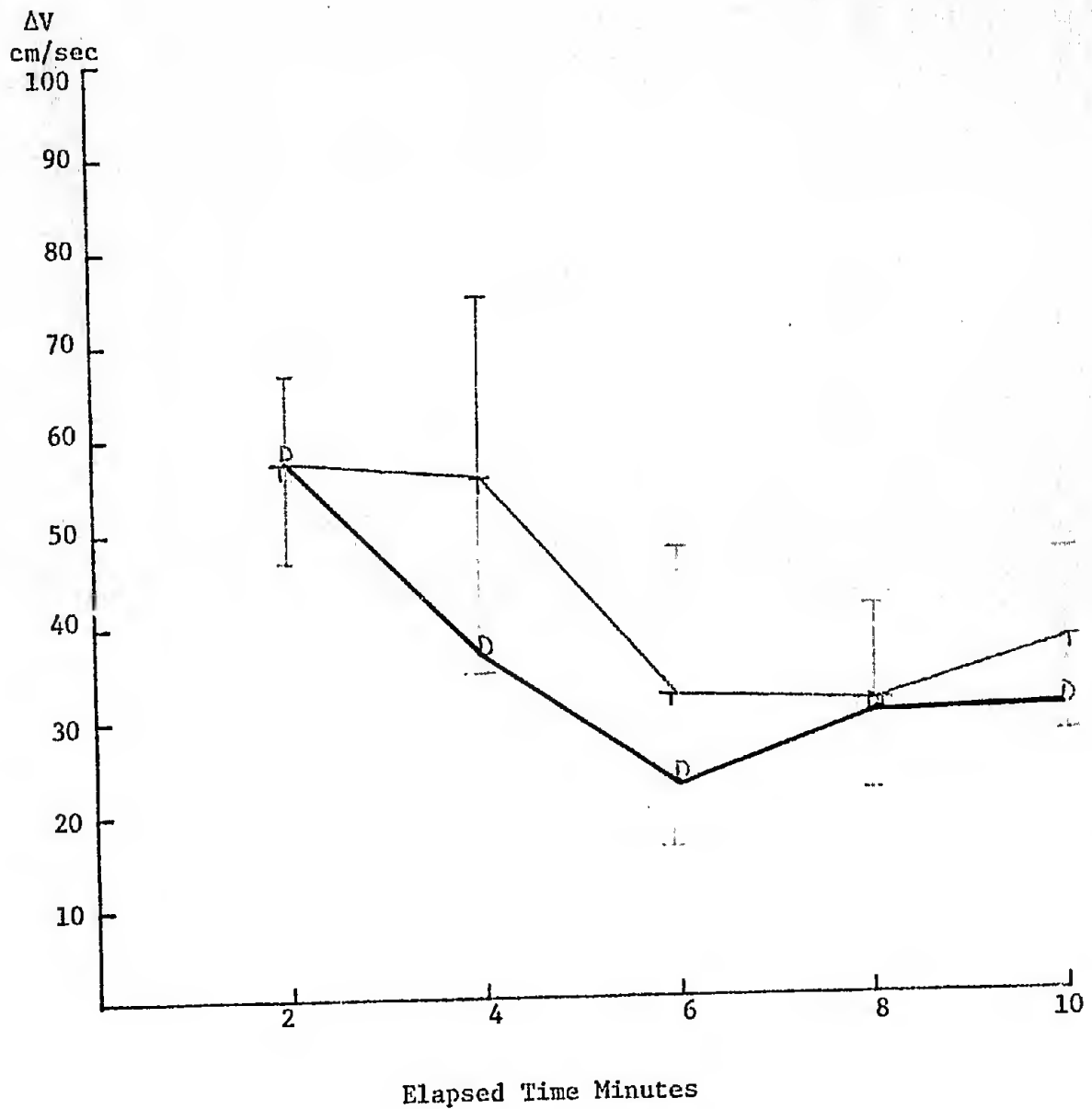


Figure 4.3. Comparison of the velocity gradient obtained from 1420 EDT two minute average wind profile measurements from the Thorntwaite anemometer (T) and two minute average of velocity gradient from the velocity gradient instrument (D). Large fluctuations of the velocity gradient obtained from the Thorntwaite are attributed to uncertainties in reading the counters accurately and determining the velocity gradient from the plotted profiles.

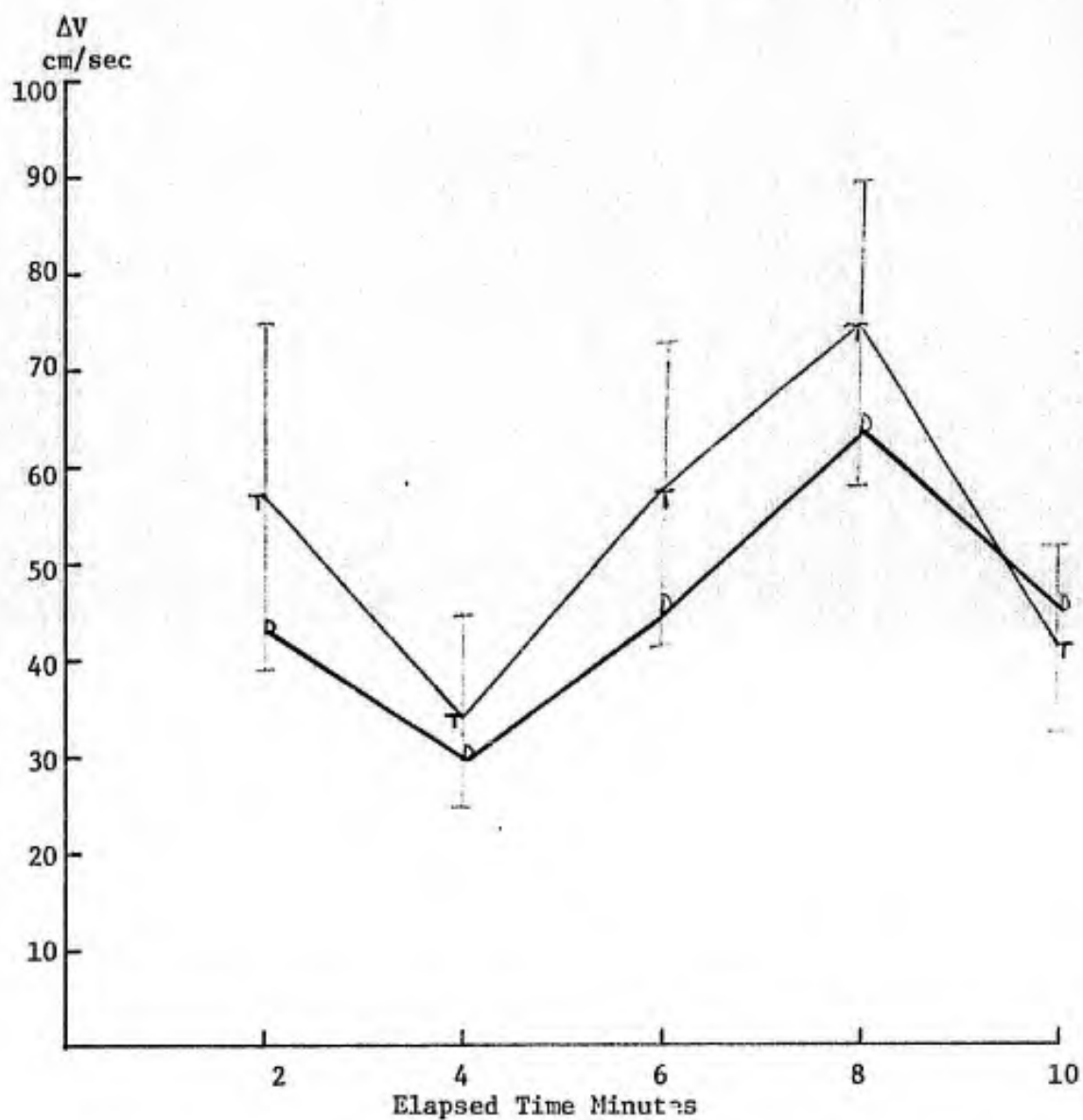


Figure 4.4. Comparison of velocity differences measured during 1510EDT run from two minute average wind profile measurements by Thornthwaite anemometer (T) and by the velocity gradient instrument (D). Limits of uncertainty for the two minute Thornthwaite anemometer values are outlined by error bias.

ΔV
Thornthwaite
Anemometer

40

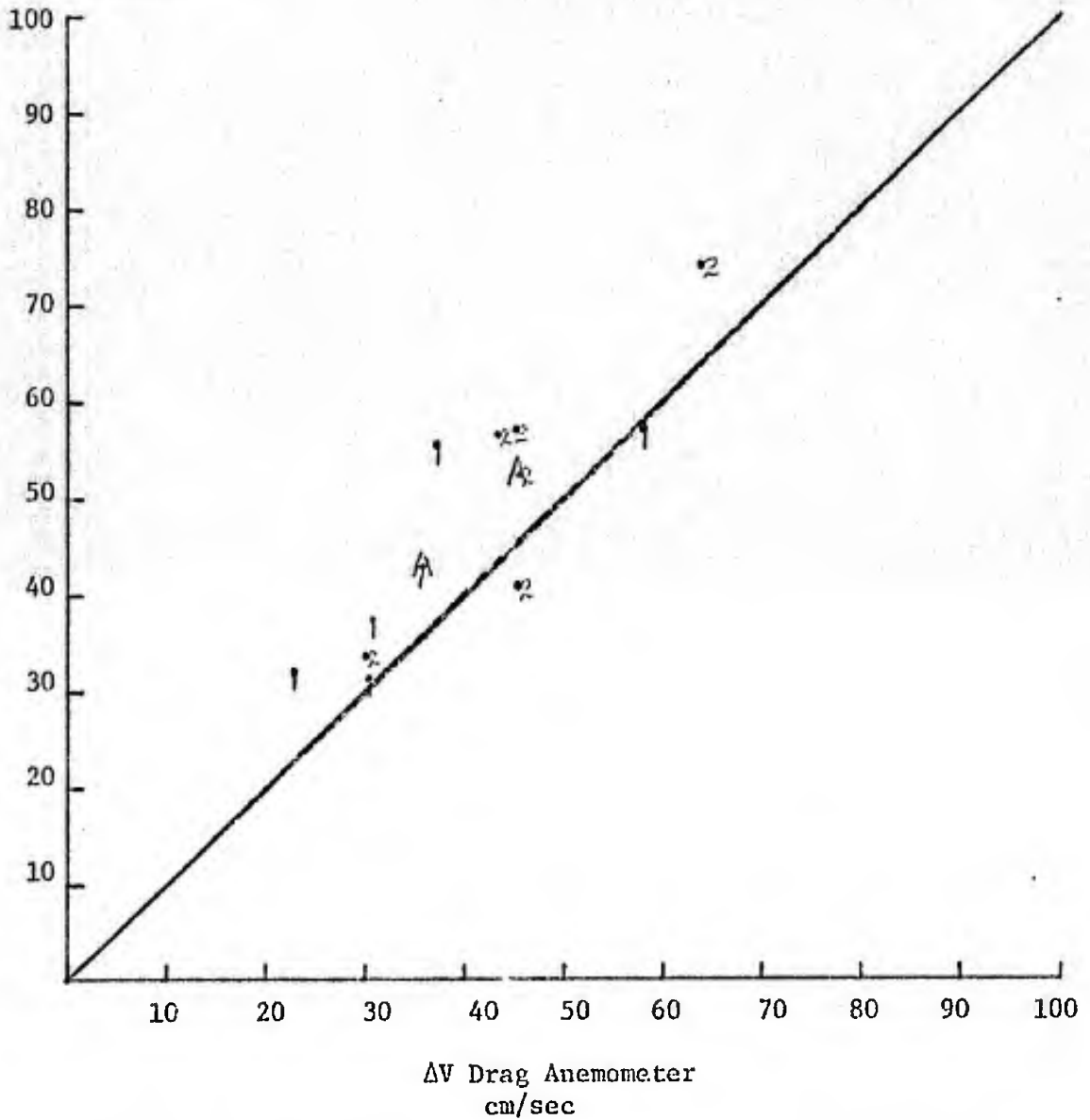


Figure 4.5. Plot of the scatter about a perfect correlation of the velocity gradient as measured by the two instruments. The averaged value for both instruments is plotted as an A. Data points from 1420 EDT are plotted as 1 and 1510 data points are plotted as 2.

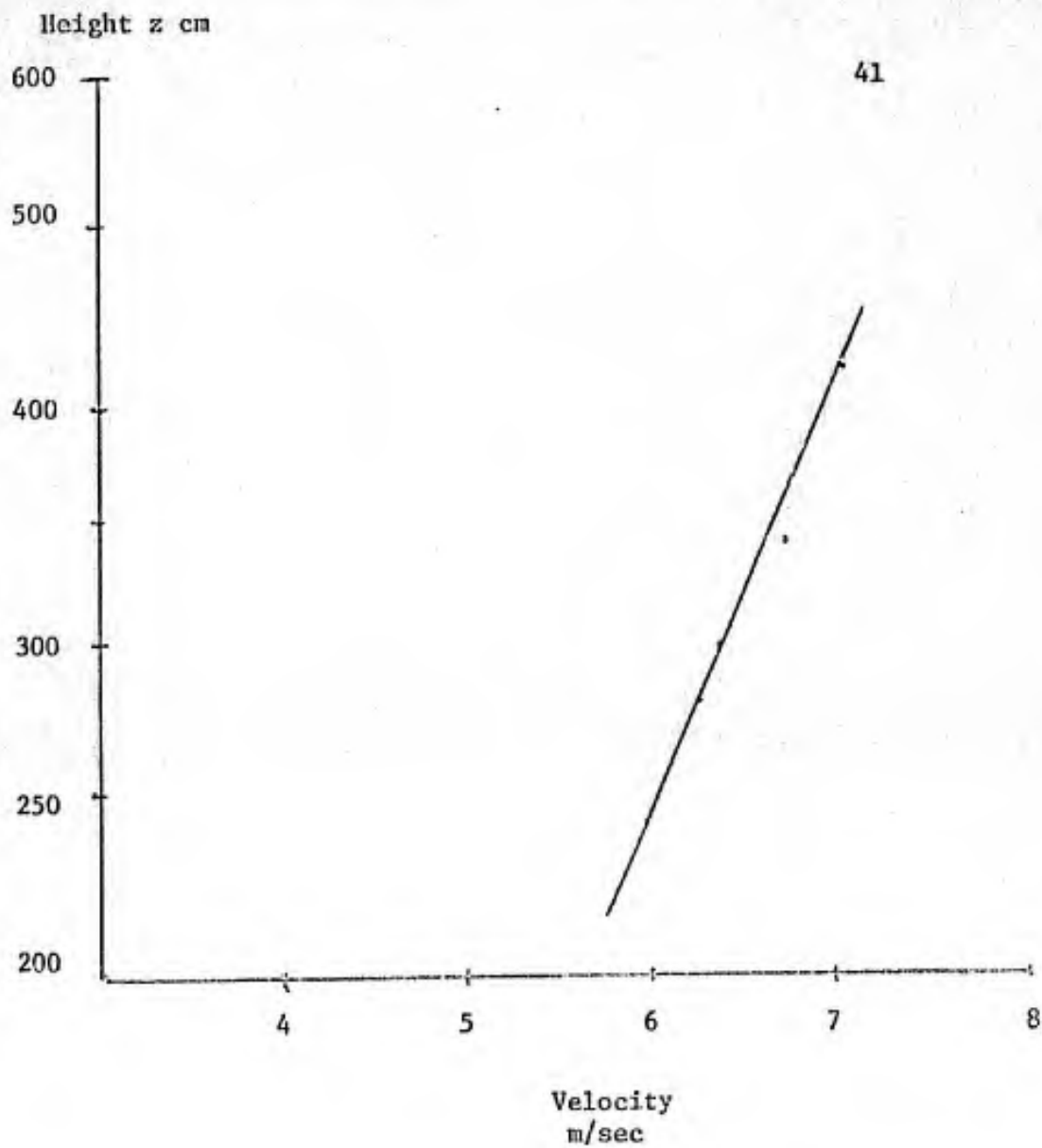


Figure 4.6. Some of the problems in extrapolating the Thornthwaite profile data for comparison of the two instruments are illustrated by observing scatter of velocity points over the graph for the 10 minute average of 1510 EDT run.

scatter arises due to uncertainties in interpreting the Thornthwaite anemometer profiles. The 10 minute average profile for the 1510 EDT run is given in Figure 4.6. It is apparent from this graph why some of the uncertainties arise. In addition the points lie predominantly to the left of the line of perfect correlation. There was a systematic, but very small, factor that data obtained from the Thornthwaite anemometer was larger than that from the drag anemometer. The average velocities measured at the center drag anemometer were 4.94 m/sec measured by the Thornthwaite and 4.83 m/sec measured by the drag during the 1420 EDT run and during the 1510 EDT run the Thornthwaite averaged 6.75 m/sec, while the drag averaged 6.44 m/sec.

5.0 SUMMARY AND CONCLUSIONS

5.1 Summary of the Problem and Procedures

The original objective was to determine the feasibility of measuring vertical gradients of horizontal velocity accurately with drag anemometers. The scope of this study was enlarged to include construction and testing of a velocity gradient instrument when it was determined feasible to use drag anemometers for sensors. The velocity gradient instrument was constructed with drag anemometers mounted on extremely sensitive wind vanes designed by Danish meteorologists for turbulence measurements. The instrument was tested by comparing its results to simultaneous velocity profiles taken by a Thorntwaite sensitive cup anemometer assembly. Results of one minute averages taken simultaneously over a 10 minute run agreed well. Ten minute overall averages for these two instruments were in excellent agreement. The greatest source of error came from reading Thorntwaite anemometer counters and interpreting those readings to obtain velocity profiles.

5.2 Limitations

The major problem which limits use of the velocity gradient instrument is its extreme sensitivity. Signals from the drag anemometers must be filtered to eliminate high frequency responses and noise or the instrument should be damped to remove resonant oscillations. Temperature compensation problems can be overcome and present no great limitation.

The greatest limitation in this experiment was comparison of the extremely sensitive drag anemometer with the Thornthwaite sensitive cup anemometer. A better comparison could have been obtained had several suitable hot wire anemometers been available.

5.3 Suggestions for Further Studies

Thermistors or diodes should be mounted on the sensor units to obtain the temperature gradient directly. This information can be combined electronically to measure directly the gradient Richardson number. The Richardson number obtained in this manner should be compared, under suitable assumptions, to that obtained from the fluxes of heat, momentum, and moisture and to that obtained by current estimates of the gradient Richardson number.

Additionally, data for coherence studies and studies of wind spectra can be readily obtained with this instrument. It was fascinating to watch the behavior of the velocity gradient as the various eddies traveled through the sensing regions.

5.4 Conclusions

A relatively inexpensive but highly sensitive velocity gradient instrument can be constructed for measurements in turbulence and diffusion using the drag anemometer. It would be more accurate and more responsive than most existing commercial anemometers. Results of comparison tests are extremely favorable but are limited mainly to the instrument used in this comparison.

REFERENCES

- Brackett, A. H., Jr., 1968: Semiconductor Strain Gages - When and How, Baldwin-Hamilton Corporation, Waltham, Mass.
- Budyko, M. I., 1974: Climate and Life, Academic Press, New York, New York.
- Busch, N. E. and S. E. Larsen, 1974: Hot-wire Measurements in the Atmosphere, Part I: Calibration and Response Characteristics, DISA Information, DISA Elektronik A/S, DK-2740 Skovlunde, Denmark.
- Chepil, W. S. and F. H. Siddoway, 1959: Strain Gage Anemometer for Analyzing Various Characteristics, Journal of Meteorology, Vol. 16: 411-418.
- DiVecchio, R., unpublished paper, 1972: Strain Gage Anemometer, The Pennsylvania State University, University Park, Pa.
- Dorsey, J., 1964: Semiconductor Strain Gage Handbook, Baldwin-Lima-Hamilton Corporation, Waltham, Mass.
- Fuchs, M. and C. B. Tanner, 1967: Evaporation from a Drying Soil, Journal of Applied Meteorology, Vol. 6: 852-857.
- Haltiner, G. J. and F. L. Martin, 1957: Dynamical and Physical Meteorology, McGraw-Hill, New York, New York.
- Norman, J. M. and D. W. Thomson, 1974: Fundamentals of Atmospheric Measurements, The Pennsylvania State University, University Park, Pa.
- Norwood, M. H., A. E. Cariffo, and V. E. Olsyewski, 1966: Drag Force Solid State Anemometer and Vane, Journal of Applied Meteorology, Vol. 5: 887-892.
- Pond, S., S. D. Smith, P. F. Hamblin, and R. W. Burling, 1966: Spectra of Velocity and Temperature Fluctuations in the Atmospheric Boundary Layer Over the Sea, Journal of Atmospheric Sciences, Vol. 23: 376-386.
- Reed, W. H., III and J. W. Lynch, 1963: A Simple Fast Response Anemometer, Journal of Applied Meteorology, Vol. 2: 412-416.
- Slade, D. B., 1968: Meteorology and Atomic Energy, 1968, U. S. Atomic Energy Commission, Oak Ridge, Tenn.
- Tanner, C. B., 1956: University of Wisconsin Soils Bulletin No. 6, University of Wisconsin, Madison, Wisconsin.

UNCLASSIFIED

SECURITY CLASSIFICATION OF THIS PAGE (When Data Entered)

REPORT DOCUMENTATION PAGE		READ INSTRUCTIONS BEFORE COMPLETING FORM
1. REPORT NUMBER CI-76-10	2. GOVT ACCESSION NO.	3. RECIPIENT'S CATALOG NUMBER
4. TITLE (and Subtitle) A SOLID STATE DRAG ANEMOMETER USED TO MEASURE VERTICAL WIND SHEAR		5. TYPE OF REPORT & PERIOD COVERED Master of Science Thesis
7. AUTHOR(s) GEORGE F. DUFFIELD CAPTAIN, USAF		6. PERFORMING ORG. REPORT NUMBER
9. PERFORMING ORGANIZATION NAME AND ADDRESS AFIT student at Pennsylvania State University University Park PA		8. CONTRACT OR GRANT NUMBER(s)
11. CONTROLLING OFFICE NAME AND ADDRESS Air Force Institute of Technology (CI) Wright-Patterson AFB OH 45433		10. PROGRAM ELEMENT, PROJECT, TASK AREA & WORK UNIT NUMBERS
14. MONITORING AGENCY NAME & ADDRESS (if different from Controlling Office)		12. REPORT DATE May 1975
		13. NUMBER OF PAGES 4 51
		15. SECURITY CLASS. (of this report) Unclassified
		15a. DECLASSIFICATION/DOWNGRADING SCHEDULE
16. DISTRIBUTION STATEMENT (of this Report) Approved for Public Release, Distribution unlimited		
17. DISTRIBUTION STATEMENT (of the abstract entered in Block 20, if different from Report)		
18. SUPPLEMENTARY NOTES <i>Jerry C. Hix</i> JERRY C. HIX, Captain, USAF Director of Information, AFIT APPROVED FOR PUBLIC RELEASE AFR 190-17.		
19. KEY WORDS (Continue on reverse side if necessary and identify by block number)		
20. ABSTRACT (Continue on reverse side if necessary and identify by block number)		

